Frontiers in Bioscience Scholar

Front. Biosci. (Schol Ed) **2025**; 17(4): 42728
https://doi.org/10.31083/FBS42728

Original Research

Uterine Fibroids-Associated GWAS Loci and the Risk of Arterial Hypertension: A Pilot Study

Liubov Ponomareva[1,2], Anna Dorofeeva[1], Julia Samoylenko[1], Ksenia Kobzeva[1], Olga Bushueva[1,3,*]

[1]Laboratory of Genomic Research, Research Institute for Genetic and Molecular Epidemiology, Kursk State Medical University, 305041 Kursk, Russia
[2]Department of Obstetrics and Gynecology, Institute of Continuing Education, Kursk State Medical University, 305041 Kursk, Russia
[3]Department of Biology, Medical Genetics and Ecology, Kursk State Medical University, 305041 Kursk, Russia
*Correspondence: olga.bushueva@inbox.ru (Olga Bushueva)
Academic Editor: Yoshinori Marunaka
Submitted: 29 May 2025 Revised: 30 July 2025 Accepted: 6 August 2025 Published: 17 December 2025

Abstract

Background: Uterine fibroids (UFs) are the most common benign tumors in women of reproductive age and are frequently associated with impaired fertility, reproductive dysfunction, and pregnancy complications. Arterial hypertension (AH) is another prevalent chronic condition in women, while increasing epidemiological evidence demonstrates the existence of a bidirectional relationship between UFs and AH. However, the genetic mechanisms underlying this association remain unclear. We hypothesized that UF-associated loci identified in genome-wide association studies (GWAS) may contribute to AH susceptibility. **Methods**: Genomic DNA from 606 hospitalized patients with UFs (n = 178 with comorbid AH; n = 428 AH-free) underwent allele-specific PCR amplification targeting 17 common GWAS-derived polymorphisms. **Results**: The rs1812266 (*LOC105375949*) locus was associated with a reduced risk of AH (odds ratio (OR) = 0.74; $p = 0.028$). Model-based multivariate dimensionality reduction (MB-MDR) analysis revealed significant gene–gene interactions ($p_{\text{perm}} \leq 0.05$) involving UF loci and AH risk, including five key variants (rs66998222, *LOC102723323*; rs2456181, *ZNF346*; rs1812266, *LOC105375949*; rs10929757, *GREB1*; rs7986407, *FOXO1*) appearing in multiple models. Notably, rs66998222 was observed in five models, suggesting this residue possesses a central role. For gene–environment interactions, five variants, rs66998222, *LOC102723323*; rs1812266, *LOC105375949*; rs10929757, *GREB1*; rs2456181, *ZNF346*; rs2553772, *LOC105376626*, appeared in multiple models, with the smoking × rs66998222 interaction being central to five models. These six risk variants subsequently underwent systematic functional annotation to characterize the potential associated biological roles. Bioinformatics analysis indicated that single nucleotide polymorphisms (SNPs) associated with oxidative stress, renin–angiotensin–aldosterone system (RAAS) function, tissue fibrosis, angiogenesis, and smooth muscle cell remodeling are common mechanisms in both UFs and AH. Cis-eQTL genes and transcription factor (TF)-linked biological processes mediate these mechanisms. Validation using the Cardiovascular Disease Knowledge Portal confirmed the relevance of several SNPs to blood pressure traits. **Conclusions**: To our knowledge, this is the first study to explore the genetic overlap between UFs and AH, providing novel molecular evidence for shared pathophysiological pathways. Our findings support the concept of a common genetic predisposition underlying both conditions and may inform new directions for integrated reproductive and cardiovascular health strategies.

Keywords: uterine fibroids; hypertension; genome wide association studies; single nucleotide polymorphism

1. Introduction

Uterine fibroids (UF) and arterial hypertension (AH) are highly prevalent conditions that exert a considerable impact on the health of women during both reproductive and postmenopausal periods [1]. UF is recognized as one of the most common benign tumors affecting women of reproductive age. According to epidemiological data, the prevalence of uterine fibroids reaches approximately 70–80%, with clinically significant symptoms observed in about 20–50% of affected individuals [2,3]. This condition is associated with a wide range of adverse outcomes, including abnormal uterine bleeding, anemia, chronic pelvic pain, reproductive dysfunction, infertility, and pregnancy-related complications [4,5]. Similarly, arterial hypertension remains one of the most widespread chronic disorders, affecting an estimated 28.5–31.1% of the global adult population [6].

AH has been frequently identified as a potential risk factor for the development of UF [7]. Moreover, growing evidence suggests a possible bidirectional relationship, indicating that UF itself may contribute to an increased risk of hypertensive disorders. Several studies have shown that the presence of UF is associated with a 1.44- to 1.88-fold higher risk of developing hypertension [8,9], as well as hypertensive complications during pregnancy, such as preeclampsia [10,11].

Despite the accumulating clinical and epidemiological data supporting an association between these conditions, the genetic underpinnings of this relationship remain largely unexplored. In recent decades, genome-wide association studies (GWAS) have emerged as a powerful approach for identifying genetic loci associated with susceptibility to various complex diseases [12]. In the context of

Table 1. Baseline characteristics of the study cohort.

Baseline characteristics of the study cohort		Patients with uterine fibroid (N = 606)		*p*-value
		With arterial hypertension (N = 178; 29.4%)	Without arterial hypertension (N = 428; 70.6%)	
Age	Me [Q1; Q3], N	51 [48; 57], 178	47 [42; 50], 428	**<0.001**
BMI	Me [Q1; Q3], N	30.2 [27; 34], 102	26.3 [23; 29.8], 178	**<0.001**
Smoking	Yes, N (%)	22 (12.4%)	68 (15.9%)	>0.05
	No, N (%)	156 (87.6%)	360 (84.1%)	
	ND, N (%)	-	-	
Age of UF diagnosis	Me [Q1; Q3], N	43 [38; 46], 133	40 [35; 44], 332	**<0.001**
Multiple form of UF	Yes, N (%)	85 (47.8%)	231 (54%)	>0.05
	No, N (%)	63 (35.4%)	141 (32.9%)	
	ND, N (%)	30 (16.9%)	56 (13.1%)	

Note: Me, median; Q1, the first quartile; Q3, the third quartile; ND, no data; BMI, body mass index; UF, uterine fibroids; differences that are statistically significant are indicated in bold.

UF, GWAS have successfully identified multiple genetic variants linked to increased disease risk [13–16]. Similarly, GWAS have also revealed numerous loci implicated in the pathogenesis of AH [17,18].

However, to date, no studies have specifically addressed whether genetic loci associated with UF risk may also influence the development of AH.

2. Materials and Methods

2.1 Study Participants

The study cohort consisted of 606 unrelated UF patients from Central Russia, including 178 hospitalized individuals with comorbid arterial hypertension and 428 normotensive controls. The Ethical Review Committee of Kursk State Medical University approved the study protocol (protocol No 5 from May 11, 2021), and all participants provided written informed consent. The study was carried out in accordance with the guidelines of the Declaration of Helsinki. The inclusion criteria for the study required participants to have self-declared Russian ancestry and to have been born in Central Russia. Table 1 provides the baseline and clinical characteristics of the study cohort.

The patients were enrolled in the study with ultrasound-verified UF from 2021 to 2023 at two tertiary care facilities (Perinatal Centre and Kursk City Maternity Hospital).

Patients with AH were selected from those with clinically confirmed systolic blood pressure $\geq$140 mmHg and/or diastolic blood pressure $\geq$90 mmHg, as well as patients taking antihypertensive drugs [19] (Table 1).

2.2 Identification and Inclusion of Environmentally Modifiable AH Risk Factors

Cigarette smoking has been conclusively linked to hypertension pathogenesis through its dual-phase impact on endothelial function and vascular tone regulation. Nicotine induces sympathetic nervous system activation, leading to vasoconstriction and increased blood pressure, while long-term exposure contributes to endothelial dysfunction and arterial stiffness [6,18].

2.3 Selection of Genes and Polymorphisms

The selection of genetic variants for this study was performed in two consecutive stages. In the initial stage, candidate single nucleotide polymorphisms (SNPs) were identified from the database - GWAS Catalog (https://www.ebi.ac.uk/gwas/; accessed March 14, 2024), which at that time contained 238 SNPs across 169 loci associated with uterine fibroid susceptibility based on 22 genome-wide association studies. Priority was given to SNPs that showed consistent associations with uterine fibroid risk in at least two independent studies of European populations. We excluded variants with minor allele frequencies below 0.05 and those that presented technical challenges for TaqMan probe design due to high GC content, GC clamps, or extended homopolymeric sequences. This initial screening process yielded seven candidate SNPs: rs72709458 (*TERT*), rs58415480 (*SYNE1*), rs7907606 (*STN1/SLK*), rs547025 (*SIRT3*), rs117245733 (*LINC00598*), rs7986407 (*FOXO1*) and rs2456181 (*ZNF346*). The second stage of SNP selection utilized the Reproductive System Knowledge Portal (https://reproductive.hugeamp.org/; accessed October 10, 2024), which provides comprehensive GWAS meta-analysis data for reproductive disorders. Using the search term "uterine fibroids", we identified additional candidate SNPs while applying the same exclusion criteria regarding minor allele frequency and technical feasibility of genotyping using fluorescent probes. This secondary analysis contributed ten additional SNPs to our study: rs66998222 (*LOC102723323*), rs59760198 (*DNM3*), rs10929757 (*GREB1*), rs9419958 (*STN1*), rs1812266 (*LOC105375949*), rs1986649 (*FOXO1*), rs641760 (*PITPNM2*), rs2235529 (*WNT4*), rs2553772

(*LOC105376626*), and rs11031731 (*THEM7P/WT1*). The combined selection process resulted in a final set of 17 SNPs that met our criteria for both established association with uterine fibroids and technical suitability for genotyping analysis. This two-phase approach allowed us to comprehensively capture genetic variants of potential importance in uterine fibroid pathogenesis while ensuring methodological robustness in our subsequent analyses.

2.4 Genetic Analysis

Genotyping procedures were conducted at the Laboratory of Genomic Research, Research Institute for Genetic and Molecular Epidemiology, Kursk State Medical University (Kursk, Russia). Venous blood samples (up to 5 mL) were collected from the cubital vein of each participant and stored in EDTA-coated tubes at –20 °C until processing. Genomic DNA was extracted using standard protocols, including phenol/chloroform extraction and ethanol precipitation, and its purity, quality, and concentration were assessed using a NanoDrop spectrophotometer (Thermo Fisher Scientific, Waltham, MA, USA).

Allele-specific real-time PCR assays, developed in-house, were used for genotyping. Primer and probe sequences were designed using Primer3web software (version 4.1.0, ELIXIR, Cambridge, MA, USA) [20]. PCR amplification was carried out in 25 µL reaction mixtures containing 1.5 units of Hot Start Taq DNA polymerase (Biolabmix, Novosibirsk, Russia), approximately 10 ng of DNA, and the following reagent concentrations: 0.25 µM of each primer; 0.1 µM of each probe; 250 µM of each dNTP; and varying $MgCl_2$ concentrations: 4 mM for rs59760198, 3 mM for rs117245733, rs547025, rs10929757, rs9419958, rs1812266, rs1986649, rs2553772 and rs11031731, 3.5 mM for rs2456181, rs7907606, rs641760 and rs2235529, 2.5 mM for rs7986407, rs58415480 and rs72709458, and 1.5 mM for rs66998222. The PCR buffer (1× concentration) contained 67 mM Tris-HCl (pH 8.8), 16.6 mM $(NH_4)_2SO_4$, and 0.01% Tween-20. The thermal cycling protocol consisted of an initial denaturation at 95 °C for 10 minutes, followed by 39 cycles of 92 °C for 30 seconds and annealing at various temperatures: 64 °C (rs117245733 *LINC00598*, rs1986649 *FOXO1*, rs2553772 *LOC105376626*, rs11031731 *THEM7P/WT1*, rs2235529 *WNT4*, rs59760198 *DNM3*), 65 °C (rs547025 *SIRT3*, rs10929757 *GREB1*, rs641760 *PITPNM2*), 63 °C (rs2456181 *ZNF346*), 62 °C (rs7907606 *STN1/SLK*), 60 °C (rs58415480 *SYNE1*, rs1812266 *LOC105375949*), 59 °C (rs7986407 *FOXO1*, rs72709458 *TERT*), 61 °C (rs9419958 *STN1*), and 66 °C (rs66998222 *LOC102723323*). For quality control, 10% of samples underwent blinded duplicate genotyping, demonstrating >99% concordance. SNPs rs9419958 (*STN1*) and rs7907606 (*STN1, SLK*), which deviated from Hardy-Weinberg equilibrium in controls, were re-genotyped and showed 100% concordance with initial results, confirming data reliability.

2.5 Statistical Analysis

The analysis of statistical data was performed using the STATISTICA software (version 13.3, StatSoft, Santa Clara, CA, USA). To assess the normality of the data distribution, the Shapiro-Wilk test was utilized. As most quantitative variables did not follow a normal distribution, the results were expressed as medians (Me) along with their corresponding interquartile ranges [Q1–Q3]. For comparing quantitative variables between two independent groups, the Mann-Whitney U test was applied. Differences in categorical variables were evaluated using Pearson's chi-squared test, with Yates' correction for continuity when appropriate.

The Hardy-Weinberg equilibrium for genotype distributions was tested using Fisher's exact test. The SNPStats web-based platform (https://www.snpstats.net/start.htm, accessed on February 7, 2025) was employed to perform logistic regression analyses examining potential correlations between genotype distributions and AH susceptibility. This analysis followed an additive genetic model and was adjusted for confounding factors, including age, body mass index (BMI) and age of UF diagnosis. To account for the influence of risk factors on genetic marker associations, separate analyses were performed for individuals with and without exposure to these factors.

The AH patient cohort and control group met the required power criteria of 80%, as calculated using the online GAS Power Calculator [21]. Analyses employed a multiplicative model with a significance level of 0.05. Given an AH prevalence of 0.08 in Central Russia and minor allele frequencies ranging from 0.07 to 0.49, the sample sizes of AH patients (n = 180) and controls (n = 430) provided sufficient power to detect intergroup differences in minor allele frequencies at OR between 1.39 and 1.8.

The analysis utilizing the model-based multivariate dimensionality reduction (MB-MDR) method investigated combinations of genotypes at two, three, and four levels, assessing both gene-gene (G×G) interactions and interactions between genotypes and AH risk factor (smoking) (gene-environment, G×E) (method was described in details in our previous studies [22]). To ensure the robustness of the results, empirical *p*-values (p_{perm}) were calculated for each model using permutation testing with 1000 iterations, which is the standard approach for evaluating all potential interactions of a given complexity. Associations demonstrating permutation-adjusted significance ($p_{perm} < 0.05$) were considered statistically reliable [23]. All regression models incorporated adjustments for three key confounders: age, BMI and age of UF diagnosis to control for potential confounders.

All statistical analyses were performed using R version 3.6.3 (R Foundation for Statistical Computing, Vienna, Austria). For every interaction tier, we retained the top three to four models exhibiting maximal Wald statistics and minimal *p*-values for subsequent evaluation. The MB-MDR method also enabled the identification of spe-

Table 2. Genetic associations between UF GWAS loci and AH susceptibility.

Genetic variant	Effect allele	Other allele	N	OR[1] (95% CI)	p^2
rs117245733 *LINC00598*	A	G	654	0.93 (0.38–2.26)	0.87
rs547025 *SIRT3*	C	T	654	0.95 (0.56–1.62)	0.86
rs2456181 *ZNF346*	C	G	653	1.14 (0.89–1.46)	0.31
rs7907606 *STN1, SLK*	G	T	654	1.06 (0.77–1.45)	0.73
rs58415480 *SYNE1*	G	C	654	0.87 (0.62–1.23)	0.43
rs7986407 *FOXO1*	G	A	653	0.97 (0.73–1.27)	0.81
rs72709458 *TERT*	T	C	653	0.95 (0.69–1.30)	0.73
rs66998222 *LOC102723323*	A	G	654	1.23 (0.92–1.65)	0.17
rs59760198 *DNM3*	T	C	650	1.17 (0.89–1.54)	0.27
rs10929757 *GREB1*	A	C	653	0.78 (0.59–1.02)	0.067
rs9419958 *STN1*	T	C	654	1.11 (0.80–1.55)	0.52
rs1812266 *LOC105375949*	C	G	654	**0.74 (0.57–0.97)**	**0.028**
rs1986649 *FOXO1*	T	C	654	1.20 (0.87–1.67)	0.27
rs641760 *PITPNM2*	T	C	652	0.88 (0.62–1.23)	0.44
rs2235529 *WNT4*	T	C	651	0.98 (0.68–1.42)	0.92
rs2553772 *LOC105376626*	T	G	653	1.11 (0.86–1.44)	0.43
rs11031731 *THEM7P, WT1*	A	G	654	1.14 (0.80–1.63)	0.46

Note: All statistical models used the minor allele as reference and controlled for age, BMI and age of UF diagnosis. Data show: [1] adjusted odds ratios with 95% CIs; [2] significance values. Bold indicates $p < 0.05$. GWAS, genome-wide association studies; AH, arterial hypertension.

cific genotype combinations significantly associated with the studied phenotypes ($p < 0.05$). These calculations were performed using the MB-MDR program compatible with R (version 3.6.3).

To explore the functional implications of the studied SNPs, several bioinformatics tools described in details in our previews studies [24] were employed:

- The GTEx Portal (http://www.gtexportal.org/, accessed on February 13, 2025) was used to analyze SNP associations with expression quantitative trait loci (eQTLs) in various tissues, including heart, vessels and blood [25].
- eQTLGen (https://www.eqtlgen.org/, accessed on February 13, 2025) provided additional data on SNP-eQTL relationships, particularly in peripheral blood samples.
- HaploReg v4.2 (https://pubs.broadinstitute.org/mammals/haploreg/haploreg.php, accessed on February 13, 2025) was utilized to examine SNP locations within regulatory elements, such as DNase hypersensitive regions, and their links to histone modifications.
- The atSNP Function Prediction tool (http://atsnp.biostat.wisc.edu/search, accessed on February 13, 2025) assessed how SNP variations affected transcription factor binding affinity based on reference and alternative alleles [26].
- Gene Ontology (http://geneontology.org/, accessed on February 13, 2025) was applied to identify biological processes enriched among transcription factors associated with the studied SNPs, connecting these processes to AH pathogenesis [27].
- The Cardiovascular Disease Knowledge Portal (CVDKP) (https://cvd.hugeamp.org/, accessed on February 13, 2025) integrated genetic association data, offering insights into SNP relationships with AH and related phenotypes, such as isolated increased systolic or diastolic blood pressure [28].

The integration of these bioinformatics tools provided a comprehensive understanding of the functional roles of the SNPs, their interactions with environmental risk factors, and their contributions to the molecular mechanisms underlying AH pathogenesis. This approach combined genetic, environmental, and computational analyses to uncover intricate patterns of disease susceptibility.

3. Results

3.1 Association of UF GWAS-Loci With Risk of AH in Russian Women

Significant inverse association with AH risk was observed for rs1812266 effect allele C (*LOC105375949*) in the combined analysis (OR = 0.74, 95% CI = 0.57–0.97, p = 0.028) (Table 2).

3.2 Gene-Gene Interactions Analysis (MB-MDR, MDR Modeling)

The MB-MDR analysis identified seven statistically significant intergenic interaction models ($p_{\text{perm}} \leq 0.05$) involving UF GWAS loci and AH risk: two two-locus, three three-locus, and two four-locus interactions (Table 3). These robust gene-gene networks incorporated nine polymorphic loci, with five key variants—rs66998222 (*LOC102723323*), rs2456181 (*ZNF346*), rs1812266 (*LOC105375949*), rs10929757 (*GREB1*), and rs7986407 (*FOXO1*)—participating in multiple interaction models, suggesting their central role in the genetic architecture of

Table 3. AH associated gene-gene interactions (MB-MDR modeling).

Gene-gene interaction models	NH	β H	WH	NL	β L	WL	Wmax	p_{perm}
The best 2-locus models of gene-gene interactions (for models with $p_{min.} < 0.001$, 1000 permutations)								
rs66998222 *LOC102723323* × **rs2456181 *ZNF346***	1	0.2311	12.12	1	–0.0886	4.527	12.12	0.016
rs1812266 *LOC105375949* × **rs66998222 *LOC102723323***	2	0.1426	11.19	1	–0.0958	5.539	11.19	0.028
The best 3-locus models of gene-gene interactions (for models with $p_{min.} < 1 \times 10^{-5}$, 1000 permutations)								
rs11031731 *THEM7P, WT1* × **rs1812266 *LOC105375949*** × **rs2456181 *ZNF346***	4	0.2155	22.75	0	NA	NA	22.75	0.003
rs2553772 *LOC105376626* × **rs10929757 *GREB1*** × **rs7986407 *FOXO1***	3	0.4620	22.04	1	–0.2773	3.706	22.04	0.015
rs10929757 *GREB1* × **rs66998222 *LOC102723323*** × **rs2456181 *ZNF346***	4	0.2550	21.06	1	–0.1211	4.361	21.06	0.016
The best 4-locus models of gene-gene interactions (for models with $p_{min.} < 1 \times 10^{-10}$, 1000 permutations)								
rs1986649 *FOXO1* × **rs1812266 *LOC105375949*** × **rs66998222 *LOC102723323*** × **rs2456181 *ZNF346***	9	0.3933	46.10	2	–0.2344	7.151	46.10	0.001
rs1812266 *LOC105375949* × rs59760198 *DNM3* × **rs66998222 *LOC102723323*** × **rs7986407 *FOXO1***	8	0.4001	45.42	2	–0.1800	6.984	45.42	0.002

Note: MB-MDR, model-based multivariate dimensionality reduction; NH, the number of interacting high-risk genotypes; β H, regression coefficient for high-risk interactions identified at the 2nd stage of analysis; WH, Wald statistics for high-risk interactions; NL, number of interacting low-risk genotypes; β L, regression coefficient for low-risk interactions identified at the 2nd stage of analysis; WL, Wald statistics for low-risk interactions; p_{perm}, permutational significance levels for models (all models are adjusted for age, BMI, age of UF diagnosis); NA, not applicable; Loci included in 2 or more best gene-gene models are indicated in bold.

AH susceptibility among UF patients. Notably, SNP rs66998222 (*LOC102723323*) appeared in five out of the seven most statistically significant interaction models, suggesting its potential central role in the genetic architecture linking UF susceptibility loci to AH risk.

The MDR method revealed several key findings (Fig. 1). First, the genetic variants included in the most significant gene-gene interaction models were predominantly characterized by antagonistic and additive effects, with the exception of SNPs rs2456181 *ZNF346* and rs10929757 *GREB1*, which demonstrated pronounced synergistic interactions. Second, the most notable individual effect was observed for rs66998222 *LOC102723323*, contributing 1.01% to the trait entropy associated with AH. Third, the individual (main) effects of the genetic variants involved in the top gene-gene interaction models (ranging from 0.38% to 1.01% of AH entropy contribution) were comparable to the effects of gene-gene interactions (0.06% to 0.64% of AH entropy contribution).

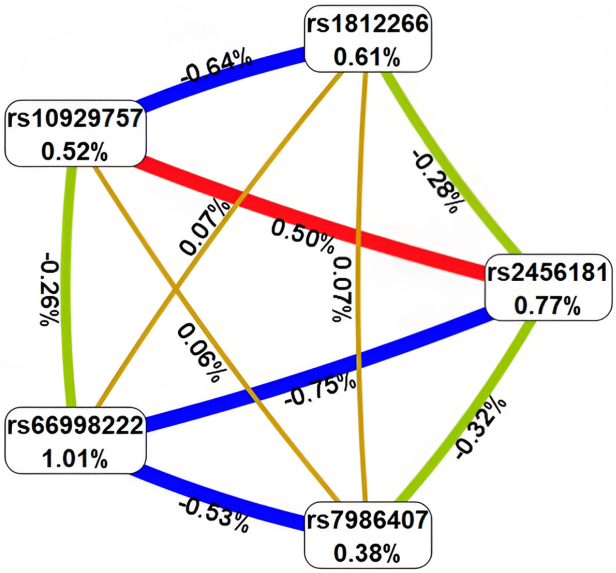

Fig. 1. Architecture of significant epistatic gene-gene networks in AH pathogenesis. Color coding: red = strongly synergistic, brown = additive interactions, green = moderate antagonistic, blue = pronounced antagonistic. Line thickness scales with effect magnitude (% entropy contribution).

Fourth, the strongest associations with AH were identified for the following genotype combinations of the polymorphic gene variants: rs66998222 *LOC102723323* (A/G) × rs2456181 *ZNF346* (C/C) (Beta = 0.231; p = 0.0005); rs1812266 *LOC105375949* (G/G) × rs66998222 *LOC102723323* (A/G) (Beta = 0.1403; p = 0.017); rs11031731 *THEM7P, WT1* (G/G) × rs1812266 *LOC105375949* (G/G) × rs2456181 *ZNF346* (C/C) (Beta = 0.2095; p = 0.007); rs2553772 *LOC105376626* (T/G) × rs10929757 *GREB1* (C/C) × rs7986407 *FOXO1* (G/G) (Beta = 0.405; p = 0.002); rs10929757 *GREB1* (C/C) × rs66998222 *LOC102723323* (A/G) × rs2456181 *ZNF346* (C/C) (Beta = 0.33; p = 0.0007); rs1986649 *FOXO1* (C/C) × rs1812266 *LOC105375949* (C/G) × rs66998222 *LOC102723323* (A/G) × rs2456181 *ZNF346* (C/C) (Beta = 0.384; p = 0.0009); rs1812266 *LOC105375949* (G/G) × rs59760198 *DNM3* (T/T) × rs66998222 *LOC102723323* (A/G) × rs7986407 *FOXO1* (A/A) (Beta = 0.499; p = 0.002) (**Supplementary Table 1**).

3.3 Gene–Environment Interactions of UF-GWAS-significant Loci Associated With AH Risk (MB-MDR and MDR Modeling)

Using the MB-MDR approach, seven most significant gene–environment interaction models associated with AH were identified, including one two-level, three three-level, and three four-level interaction models (Table 4). In total, six genetic variants were involved in the top SNP–smoking interaction models, with five of them—rs66998222 (*LOC102723323*), rs1812266 (*LOC105375949*), rs10929757 (*GREB1*), rs2456181 (*ZNF346*), and rs2553772 (*LOC105376626*)—appearing in two or more of the most significant G×E models. Notably, the interaction between smoking × rs66998222 (*LOC102723323*) served as a central component in five out of the seven most significant genotype–environment interactions associated with AH.

In the next stage of the analysis, interactions between these genetic variants and risk factors were further evaluated using Multifactor Dimensionality Reduction (MDR) modeling (Fig. 2). First, MDR analysis demonstrated that smoking, as an environmental risk factor, exhibited the weakest individual effect, contributing only 0.15% to AH-related entropy, which is considerably lower compared to the individual effects of SNPs (ranging from 0.52% to 1.01%). Second, smoking displayed heterogeneous interaction patterns with the genetic variants involved in the top gene–environment interaction models: a moderate synergistic effect in interaction with rs10929757 (*GREB1*), a moderate antagonistic effect with rs2456181 (*ZNF346*), and additive effects with rs66998222 (*LOC102723323*) and rs1812266 (*LOC105375949*).

Third, the strongest associations with AH were observed for the following gene–environment interaction combinations: no smoking × rs66998222 *LOC102723323* (A/G) (Beta = 0.135; p = 0.002); no smoking × rs1812266 *LOC105375949* (G/G) × rs66998222 *LOC102723323* (A/G) (Beta = 0.192; p = 0.005); no smoking × rs10929757 *GREB1* (C/C) × rs2456181 *ZNF346* (C/C) (Beta = 0.18; p = 0.018); no smoking × rs2553772 *LOC105376626* (T/G) × rs66998222 *LOC102723323* (A/G) (Beta = 0.159; p = 0.006); no smoking × rs1812266 *LOC105375949* (C/G) × rs66998222 *LOC102723323* (A/G) × rs2456181 *ZNF346* (C/C) (Beta = 0.485; p = 0.00001); no smoking × rs10929757 *GREB1* (C/C) × rs66998222 *LOC102723323* (A/G) × rs2456181 *ZNF346* (C/C) (Beta = 0.385; p = 0.0004); smoking × rs2553772 *LOC105376626* (T/T) ×

Table 4. Gene-environmental interactions, associated with AH (MB-MDR modeling).

Gene-gene interaction models	NH	β H	WH	NL	β L	WL	Wmax	p_{perm}
The best two-order models of gene-smoking interactions (for G×E models with $p_{min.} < 0.01$, 1000 permutations)								
SMOKE × **rs66998222** ***LOC102723323***	1	0.1353	9.40	1	–0.07	3.071	9.395	0.022
The best three-order models of gene- interactions (for G×E models with $p_{min.} < 5 \times 10^{-4}$, 1000 permutations)								
SMOKE × **rs1812266** ***LOC105375949*** × **rs66998222** ***LOC102723323***	2	0.1854	15.35	1	–0.165	2.779	15.35	0.028
SMOKE × **rs10929757** ***GREB1*** × **rs2456181** ***ZNF346***	3	0.1636	14.49	2	–0.138	6.883	14.49	0.03
SMOKE × **rs2553772** ***LOC105376626*** × **rs66998222** ***LOC102723323***	2	0.1758	13.35	2	–0.137	8.545	13.35	0.032
The best four-order models of gene- interactions (for G×E models with $p_{min.} < 1 \times 10^{-7}$, 1000 permutations)								
SMOKE × **rs1812266** ***LOC105375949*** × **rs66998222** ***LOC102723323*** × **rs2456181** ***ZNF346***	4	0.3465	31.49	1	–0.235	3.881	31.49	0.005
SMOKE × **rs10929757** ***GREB1*** × **rs66998222** ***LOC102723323*** × **rs2456181** ***ZNF346***	5	0.2809	30.11	1	–0.299	2.972	30.11	0.009
SMOKE × **rs2553772** ***LOC105376626*** × **rs10929757** ***GREB1*** × rs7986407 *FOXO1*	4	0.5388	29.79	1	–0.297	3.363	29.79	0.013

Abbreviations: SMOKE, Smoking; NH, number of high-risk genotype interactions; β H, high-risk interaction coefficient; WH, high-risk Wald statistic; NL, low-risk interaction count; β L, low-risk coefficient; WL, low-risk Wald statistic; p_{perm}, permutation-adjusted p-value. All models adjusted for age, BMI, age of UF diagnosis. Loci participating in multiple optimal G×E models are bolded.

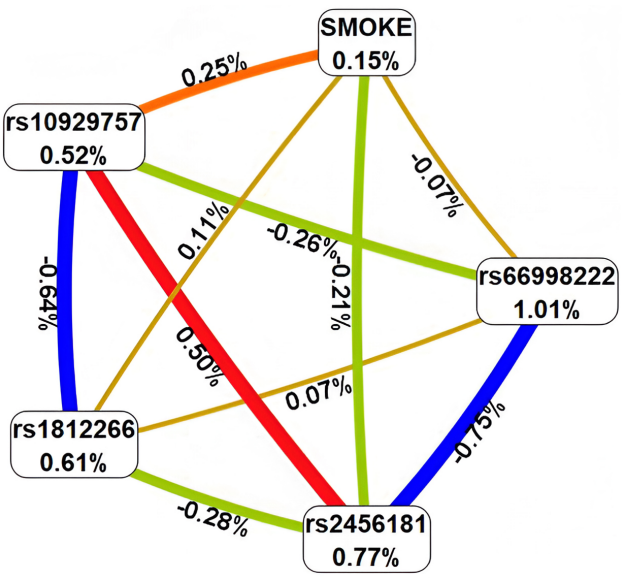

Fig. 2. Architecture of significant G×E interactions in AH pathogenesis. Color coding: SMOKE = smoking, red = strongly synergistic, orange = moderate synergistic, green = moderate antagonistic, blue = pronounced antagonistic, brown = additive effects. Line thickness corresponds to effect size (% entropy contribution).

rs10929757 *GREB1* (C/A) × rs7986407 *FOXO1* (A/A) (Beta = 0.46; p = 0.044) (**Supplementary Table 2**).

3.4 Bioinformatic Annotation of AH-linked Polymorphisms

Our integrated analysis of genetic variants, epistatic interactions, and gene-environment effects revealed significant associations between arterial hypertension and six UF-associated GWAS loci: rs2456181 *ZNF346*, rs7986407 *FOXO1*, rs66998222 *LOC102723323*, rs10929757 *GREB1*, rs1812266 *LOC105375949* and rs2553772 *LOC105376626*. These risk variants subsequently underwent systematic functional annotation to characterize their potential biological roles.

3.4.1 QTL-Effects

The results of the cis-eQTL analysis (Table 5), shed light on the impact of specific genetic variants on gene expression. According to the GTEx Portal, rs2456181 *ZNF346* increases expression of *FGFR4* and *UIMC1* in blood and arteries, and also increases *UIMC1* in heart. In the same time rs2456181 *ZNF346* increases expression itself in arteries. SNP rs7986407 *FOXO1* increases expression of *ENSG00000287837* in blood, arteries and heart and SNP decreases expression of *SLC25A15* in arteries and heart. And, lastly, SNP rs2553772 *LOC105376626* increases expression of *CD44* and *ENSG00000255521* in arteries; and SNP decreases *ENSG00000289526* in blood and *APIP* in heart.

The eQTLGen Browser data further demonstrated significant expression quantitative trait loci associations in blood samples. The rs2456181 variant in *ZNF346* was associated with decreased expression of *ZNF346-IT1* alongside increased expression levels of *UIMC1*, *FGFR4*, and *HK3*. Similarly, rs7986407 in *FOXO1* showed correlations with reduced *MRPS31*, *SLC25A15*, and *KBTBD7* expression, while exhibiting elevated expression of *WBP4* and *FOXO1* itself. Finally, the rs2553772 polymorphism in *LOC105376626* displayed positive associations with *CD44* expression but negative correlations with *RP1-68D18.4* levels (Table 5).

3.4.2 Transcription Factors

The analysis of transcription factors revealed that the SNP allele G rs2456181 *ZNF346* creates DNA binding sites for 45 TFs, co-controlling response to interleukin-9-mediated signaling pathway (GO:0038113; false discovery rate (FDR) = 1.04×10^{-2}); growth hormone receptor signaling pathway via Janus kinase/signal transducer and activator of transcription (JAK-STAT) (GO:0060397; FDR = 1.72×10^{-2}); cellular response to interleukin-17 (GO:0097398; FDR = 2.91×10^{-2}); positive regulation of vascular endothelial growth factor production (GO:0010575; FDR = 2.42×10^{-3}); cell surface receptor signaling pathway via JAK-STAT (GO:00007259; FDR = 1.55×10^{-2}); positive regulation of angiogenesis (GO:0045766; FDR = 1.57×10^{-2}) (**Supplementary Table 3**).

The ref allele A rs7986407 *FOXO1* creates DNA binding sites for 37 TFs, co-controlling response to peroxisome proliferator activated receptor signaling pathway (GO:0035357; FDR = 1.06×10^{-2}); cardiac muscle cell myoblast differentiation (GO:0060379; FDR = 1.26×10^{-2}); retinoic acid receptor signaling pathway (GO:0048384; FDR = 5.67×10^{-4}); positive regulation of apoptotic process (GO:0043065; FDR = 4.95×10^{-2}) (**Supplementary Table 4**).

The analysis of transcription factors revealed that the SNP allele A rs66998222 *LOC102723323* creates DNA binding sites for 28 TFs, co-controlling cellular response to cytokine stimulus (GO:0071345; FDR = 1.07×10^{-2}). Ref allele G rs66998222 *LOC102723323* creates DNA binding sites for 24 TFs, co-controlling regulation of interleukin-1 beta production (GO:0032651; FDR = 2.29×10^{-2}), response to hypoxia (GO:0001666; FDR = 3.02×10^{-2}) and positive regulation of cytokine production (GO:0001819; FDR = 1.90×10^{-2}) (**Supplementary Table 5**).

SNP allele C rs10929757 *GREB1* creates DNA binding sites for 44 TFs, co-controlling response to cardiac chamber formation (GO:0003207; FDR = 2.21×10^{-2}); atrioventricular canal development (GO:0036302; FDR = 2.95×10^{-2}); interleukin-6-mediated signaling pathway (GO:0070102; FDR = 3.31×10^{-2}); heart valve formation (GO:0003188; FDR = 3.59×10^{-2}); cardiac left ventricle morphogenesis (GO:0003214; FDR = 3.89×10^{-2}); regulation of cell proliferation involved in heart morphogenesis (GO:2000136; FDR = 4.30×10^{-2}); atrioventricular

Table 5. Cis-eQTL mediated gene expression modulation by AH-linked GWAS SNPs (GTEx Portal and eQTL Gene Data).

Genetic variant	Expressed gene	*p*	Effect (NES)	Tissue	Symbol	Z-score	FDR
	GTEx Portal				eQTLGene		
rs2456181 *ZNF346*(C/**G**)	*FGFR4*	1.9×10^{-12}	0.27	Whole Blood	*UIMC1*	34.953	0
	FGFR4	9.7×10^{-12}	0.27	Artery - Tibial	*FGFR4*	13.916	0
	UIMC1	6.4×10^{-7}	0.10	Artery - Tibial	*ZNF346-IT1*	–4.477	0.02
	FGFR4	9.6×10^{-7}	0.23	Artery - Aorta	*HK3*	4.279	0.047
	UIMC1	1.2×10^{-6}	0.074	Whole Blood			
	UIMC1	6.2×10^{-6}	0.12	Heart - Atrial Appendage			
	ZNF346	2.3×10^{-5}	0.13	Artery - Tibial			
*rs7986407 FOXO1 (A/**G**)*	*SLC25A15*	2.5×10^{-12}	–0.27	Artery - Tibial	*MRPS31*	–13.189	0
	ENSG00000287837	7.4×10^{-12}	0.25	Artery - Tibial	*WBP4*	7.614	0
	ENSG00000287837	1.1×10^{-10}	0.24	Whole Blood	*SLC25A15*	–5.603	0.0001
	ENSG00000287837	4.9×10^{-8}	0.27	Artery - Aorta	*FOXO1*	5.526	0.0001
	SLC25A15	5.0×10^{-7}	–0.17	Heart - Left Ventricle	*KBTBD7*	–4.391	0.029
	ENSG00000287837	1.2×10^{-6}	0.21	Heart - Atrial Appendage			
	ENSG00000287837	6.8×10^{-6}	0.20	Heart - Left Ventricle			
	SLC25A15	0.8×10^{-5}	–0.18	Heart - Atrial Appendage			
	SLC25A15	1.4×10^{-5}	–0.22	Artery - Aorta			
*rs2553772 LOC105376626 (G/**T**)*	*CD44*	5.3×10^{-35}	0.28	Artery - Tibial	*RP1-68D18.4*	–5.205	0.001
	CD44	9.2×10^{-13}	0.22	Artery - Aorta	*CD44*	4.609	0.011
	ENSG00000255521	1.3×10^{-9}	0.24	Artery - Tibial			
	CD44	1.7×10^{-6}	0.18	Artery - Coronary			
	ENSG00000289526	4.1×10^{-6}	–0.17	Whole Blood			
	APIP	0.1×10^{-5}	–0.27	Heart - Atrial Appendage			

Effect alleles appear in bold. Key terms: eQTL, expression quantitative trait loci; NES, normalized effect size; FDR, false discovery rate.

valve development (GO:0003171; FDR = 3.87×10^{-3}); regulation of cardiac muscle tissue growth (GO:0055021 FDR = 1.54×10^{-2}); ventricular septum development (GO:0003281; FDR = 3.33×10^{-2}); cardiocyte differentiation (GO:0035051; FDR = 8.37×10^{-3}); cardiac muscle tissue development (GO:0048738; FDR = 3.67×10^{-2}); response to hypoxia (GO:0001666; FDR = 1.79×10^{-2}); muscle structure development (GO:0061061; FDR = 4.47×10^{-3}); regulation of cytokine production (GO:0001817; FDR = 7.00×10^{-3}). Reference allele A rs10929757 *GREB1* creates DNA binding sites for 13 TFs, co-controlling positive regulation of apoptotic process (GO:0043065; FDR = 3.13×10^{-2}) (**Supplementary Table 6**).

The SNP allele C rs1812266 *LOC105375949* creates DNA binding sites for 29 TFs, co-controlling response to interleukin-4-mediated signaling pathway (GO:0035771; FDR = 5.94×10^{-3}); growth hormone receptor signaling pathway via JAK-STAT (GO:0060397; FDR = 1.29×10^{-2}); SMAD protein signal transduction (GO:0060395; FDR = 7.02×10^{-4}); cell surface receptor signaling pathway via JAK-STAT (GO:0007259; FDR = 9.49×10^{-3}). The Ref allele G rs1812266 *LOC105375949* creates DNA binding sites for 41 TFs, co-controlling response to cardiac muscle cell myoblast differentiation (GO:0060379; FDR = 1.19×10^{-2}); cardiac chamber formation (GO:0003207; FDR = 1.18×10^{-2}); cardiac left ventricle morphogenesis (GO:0003214; FDR = 2.11×10^{-2}); positive regulation of cardiac muscle cell proliferation (GO:0060045; FDR = 4.20×10^{-2}); cardiac muscle cell proliferation (GO:0060038; FDR = 4.51×10^{-2}); regulation of cardiocyte differentiation (GO:1905207; FDR = 4.49×10^{-2}); regulation of interleukin-2 production (GO:0032663; FDR = 1.16×10^{-2}); vasculogenesis (GO:0001570; FDR = 1.46×10^{-2}) (**Supplementary Table 7**).

SNP allele G rs2553772 *LOC105376626* creates DNA binding sites for 20 TFs, jointly involved in positive regulation of cholesterol biosynthetic process (GO:0045542; FDR = 3.67×10^{-3}); SREBP signaling pathway (GO:0032933; FDR = 4.45×10^{-3}), cellular response to transforming growth factor beta stimulus (GO:0071560; FDR = 3.01×10^{-2}). Reference allele T rs2553772 *LOC105376626* creates DNA binding sites for 42 TFs, regulating the following biological processes: cardiac muscle tissue regeneration (GO:0061026; FDR = 1.37×10^{-3}); atrioventricular node development (GO:0003162; FDR = 6.08×10^{-3}); cardiac right ventricle morphogenesis (GO:0003215; FDR = 3.46×10^{-4}); aortic valve morphogenesis (GO:0003180; FDR = 2.36×10^{-3}); negative regulation of cardiac muscle hypertrophy (GO:0010614; FDR = 3.62×10^{-2}); positive regulation of vascular endothelial growth factor production (GO:0010575; FDR = 4.19×10^{-2}); cardiac muscle hypertrophy (GO:0003300; FDR = 4.65×10^{-2}); regulation of cardiac muscle tissue growth (GO:0055021; FDR = 4.90×10^{-3}); cardiocyte differentiation (GO:0035051; FDR = 3.40×10^{-2}); positive regulation of angiogen-

esis (GO:0045766; FDR = 6.25×10^{-3}); muscle organ development (GO:0007517; FDR = 4.36×10^{-2}) (**Supplementary Table 8**).

3.4.3 Histone Modification Patterns at Identified Risk Loci

Epigenetic profiling using HaploReg v4.2 revealed characteristic histone modification patterns at AH-associated risk loci. The SNPs rs2456181 (*ZNF346*), rs7986407 (*FOXO1*), rs10929757 (*GREB1*), and rs2553772 (*LOC105376626*) consistently showed active chromatin marks in blood and cardiac tissue, including H3K4me1 (histone H3 lysine 4 mono-methylation), H3K27ac (lysine 27 acetylation), and H3K9ac (lysine 9 acetylation). Notably, rs2456181, rs7986407, and rs2553772 additionally demonstrated similar regulatory histone signatures in vascular tissues (**Supplementary Table 9**).

3.4.4 Bioinformatic Exploration of AH-associated Variants and Phenotypic Correlations

The Cardiovascular Disease Knowledge Portal confirms that two GWAS-significant variants identified in our study—rs2456181 *ZNF346* and rs1812266 *LOC105375949*—demonstrate established associations with elevated arterial hypertension risk in prior research, corroborating our findings. Moreover, rs2456181 *ZNF346* increases and rs66998222 *LOC102723323* decreases systolic blood pressure. Also, rs7986407 *FOXO1* increases and rs66998222 *LOC102723323* decreases diastolic blood pressure (**Supplementary Table 10**).

4. Discussion

Studies have demonstrated that UF is associated with a 1.44- to 1.88-fold increased risk of AH [8,9], as well as with a higher likelihood of hypertensive pregnancy disorders, including preeclampsia [10,11]. Conversely, an elevated risk of UF has also been reported among individuals with AH [7].

Both conditions share common pathophysiological features involving alterations in smooth muscle cells (SMCs). In UF, changes occur in both the myometrial tissue and vascular SMCs, whereas AH is also characterized by profound structural and functional changes in vascular SMCs [29]. According to recent findings, patients with UF exhibit alterations in arteriolar architecture, including mitochondrial and endoplasmic reticulum stress, as well as myocyte migration, which may potentially influence blood pressure regulation [30].

It is well established that components involved in blood pressure regulation, such as the renin-angiotensin-aldosterone system (RAAS) [31], may influence the risk of UF development through mechanisms associated with inflammation, cellular proliferation, angiogenesis, and fibrosis [32,33]. These processes represent common pathogenic pathways linking UF and AH [34,35].

Moreover, alterations in estrogen levels, which play a critical role in the pathogenesis of UF [36–39], are also involved in the regulation of postmenopausal vasomotor symptoms, including blood pressure modulation [40].

Given these shared pathophysiological mechanisms and accumulating clinical evidence supporting the association between UF and AH, it is plausible to assume that these two conditions are not only interrelated but may also mutually exacerbate each other.

In our study, we first evaluated the association between 17 confirmed GWAS loci associated with UF and the risk of AH. We found that rs1812266 (*LOC105375949* G/C) was associated with a decreased risk of AH (OR = 0.74, 95% CI = 0.57–0.97, $p = 0.028$). Our findings are supported by bioinformatics data from the Cardiovascular Disease Knowledge Portal (CVDKP), which aggregates data from meta-analyses of GWAS studies worldwide. According to CVDKP, six studies showed an association between rs1812266 (*LOC105375949* G/C) and a decreased risk of AH (**Supplementary Table 11**).

Bioinformatics analysis revealed that the C allele of the SNP, which showed protective effects regarding AH risk in our study, generates binding sites for transcription factors (TFs) involved in the regulation of processes such as «interleukin-4-mediated signaling pathway», which plays a key role in suppressing pro-inflammatory responses, reducing vascular damage, and improving vascular function [41]. Additionally, the C allele is involved in the JAK-STAT pathway, activated by growth hormone or cytokine receptors (e.g., IL-6, Angiotensin II). The pathway regulates cardiomyocyte hypertrophy and inflammatory processes, suggesting their role in cardiovascular pathology risk, including AH [42,43]. Moreover, the C allele of this SNP regulates "SMAD protein signal transduction" which reduces fibrotic damage in vascular SMCs [44].

Furthermore, our study demonstrated that UF-GWAS significant loci, such as rs2456181 (*ZNF346*), rs7986407 (*FOXO1*), rs66998222 (*LOC102723323*), rs10929757 (*GREB1*), and rs2553772 (*LOC105376626*), were involved in the most significant gene–gene interactions associated with the development of AH.

Functional annotation revealed that rs2456181 *ZNF346*, through cis-eQTL effects, influences the expression of several genes involved in the regulation of cardiovascular system function. Specifically, rs2456181 increases the expression of genes such as *FGFR4*, *UIMC1*, and *HK3* in blood, arteries, and the heart, while concurrently reducing the expression of *ZNF346-IT1*. The *FGFR4* gene (fibroblast growth factor receptor 4) is involved in cell proliferation and angiogenesis, and its increased expression can contribute to vascular dysfunction and AH [45,46]. The *UIMC1* gene (ubiquitin interaction motif containing 1) plays a role in the DNA damage response and cell cycle regulation, and is closely associated with menopause [47]. This could impact endothelial function,

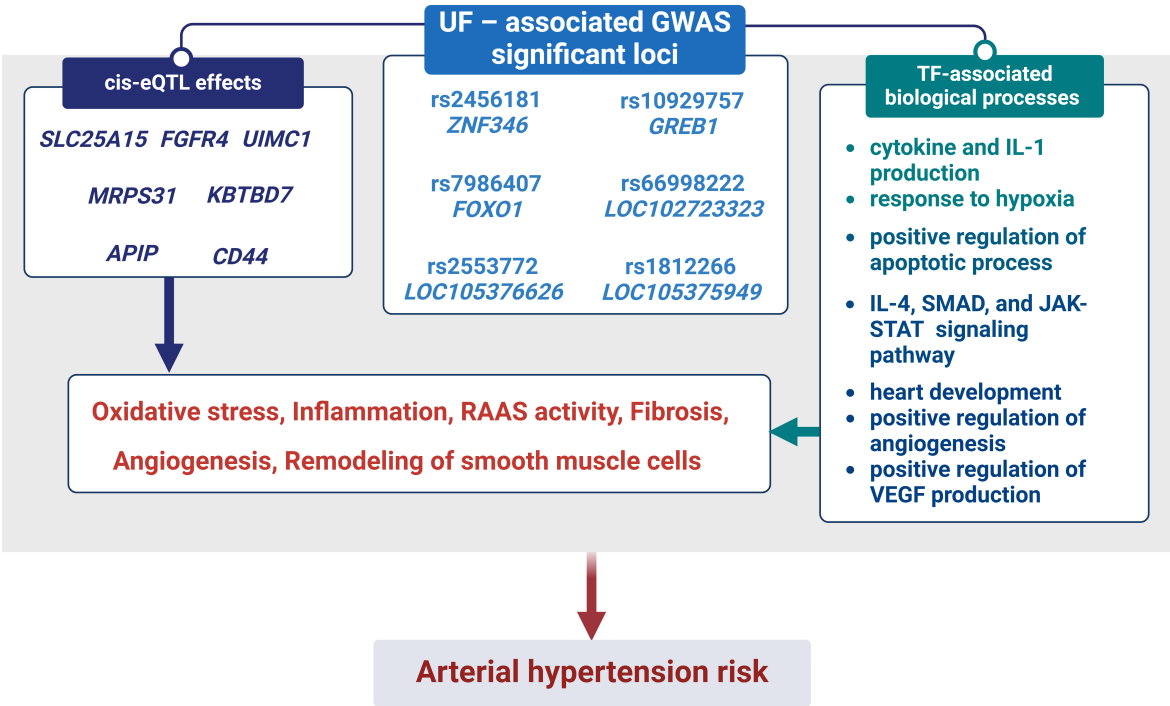

Fig. 3. The outline of associations UF-GWAS SNPs and AH risk: biological processes associated with TFs and cis-eQTL effects binding to GWAS SNPs. Notes: RAAS, renin-angiotensin-aldosterone system; TF, transcription factors; IL, interleukin; SMAD, a family of proteins that act as signal transducers in the transforming growth factor beta (TGF-β) signaling pathway; JAK-STAT, a signaling pathway, specifically the Janus kinase/signal transducer and activator of transcription pathway; VEGF, vascular endothelial growth factor.

vascular remodeling, and, ultimately, increase the risk of AH [48]. The *HK3* gene (hexokinase 3) is involved in glucose metabolism [49], and its dysregulation may be associated with metabolic disorders, which are often linked to AH [50]. The G allele (major in our case) of rs2456181 forms binding sites for transcription factors that regulate processes are likely connected to the common pathophysiological pathways of UF and AH, such as inflammation, endothelial dysfunction, and vascular remodeling [29,30]. For instance, IL-9 and IL-17 are pro-inflammatory cytokines that may amplify inflammation and promote the development of AH [51]. Data from the CVDKP confirm that the G allele of rs2456181 is associated with an increased risk of AH and an isolated increase in systolic blood pressure.

The *FOXO1* gene (forkhead box O1) regulates the cell cycle, apoptosis, oxidative stress, and vascular homeostasis [52] and may contribute to heart hypertrophy and vascular remodeling, linking it to AH [53]. Functional analysis revealed that rs7986407 (*FOXO1*), involved in the most significant gene-gene interactions, affects the expression of several genes potentially involved in the development of AH. According to cis-eQTL analysis, rs7986407 reduces the expression of *SLC25A15* (mitochondrial ornithine transporter) in arteries and the heart. The *SLC25A15* gene plays a role in nitrogen metabolism and mitochondrial function [54,55], and its reduced expression may be associated with disturbances in energy metabolism and oxidative stress, which are characteristic of AH [56–59]. Furthermore, the locus correlates with decreased expression of *MRPS31* (mitochondrial ribosomal protein) and *KBTBD7* (a protein involved in ubiquitination), as well as increased expression of *WBP4* (Wnt signaling pathway-binding protein). The *MRPS31* gene is involved in mitochondrial ribosome biogenesis, and its dysregulation may affect the energy balance of cells [60]. *WBP4* gene dysfunction has been linked to the development of neurodevelopmental syndrome with hypotonia as a symptom [61]. *KBTBD7* gene has been shown in mice experiments to influence inflammation and dysfunction in the myocardium [62]. According to the CVDKP, the G allele of rs7986407 (*FOXO1*) is associated with an increase in diastolic blood pressure, confirming its potential role in regulating vascular tone and the risk of AH.

The *LOC102723323* gene is a long non-coding RNA (lncRNA) whose function is not fully understood. However, it is known that lncRNAs can play a significant role in regulating gene expression, including genes associated with the cardiovascular system [63]. Functional analysis revealed its potential influence on cytokine pathways and the hypoxia response. The minor SNP allele A (rs66998222 *LOC102723323*), involved in forming the best gene-gene interaction models, creates binding sites for transcription factors that regulate inflammatory processes, which play a key role in the pathogenesis of AH [51,64]. According to data from the Cardiovascular Disease Knowledge Portal, the A allele of rs66998222 is associated with a reduction in

both systolic and diastolic blood pressure, highlighting its potential protective role in regulating vascular tone.

The *GREB1* gene (growth regulation by estrogen in breast cancer 1) is known for its role in regulating cell proliferation and apoptosis, as well as being a target of estrogen-dependent signaling, influencing blood pressure [65]. Functional analysis revealed that the A allele (rs10929757 *GREB1*), involved in the most significant gene-gene interactions, forms binding sites for transcription factor "positive regulation of apoptotic process", a key factor in vascular wall remodeling [30]. The C allele (SNP rs10929757), on the other hand, creates binding sites for transcription factors that control the development of heart compartments, regulation of cytokine production and response to hypoxia. IL-6 is a key pro-inflammatory cytokine that can contribute to endothelial dysfunction and vascular inflammation, characteristic of AH [66]. The response to hypoxia also plays a crucial role in regulating blood pressure through the activation of HIF-1α (hypoxia-inducible factor) and related pathways [67].

According to the cis-eQTL analysis, rs2553772 *LOC105376626*, also involved in the most significant gene-gene interactions, increases the expression of *CD44* in arteries and blood, and decreases the expression of *APIP* in the heart. The *CD44* gene encodes the hyaluronan receptor and may contribute to the pathogenesis of AH through endothelial-mesenchymal transition and inflammatory processes [68,69]. The *APIP* gene (adenosine deaminase acting on RNA) is associated with cardioprotective function [70]. The reference (minor in our case) allele T (rs2553772) forms binding sites for transcription factors that regulate crucial processes for maintaining cardiovascular homeostasis and may be linked to the pathogenesis of AH [51]. The G allele (rs2553772) creates binding sites for transcription factors controlling SREBP and TGF-β signalling pathways and play significant roles in regulating lipid metabolism and fibrosis, which may influence the development of vascular stiffness and AH [71,72].

Summarizing the findings above, we conclude that SNPs influence the risk of hypertension by affecting inflammation, response to oxidative stress, RAAS function, tissue fibrosis, angiogenesis, and SMCs remodeling. These effects are mediated through cis-eQTL interactions and biological processes related to transcription factors (Fig. 3).

5. Conclusions

For the first time, our team analyzed the relationship between GWAS loci of UF and the risk of AH, which allows for a fundamental confirmation of previously identified clinical correlations [7–9]. The obtained results may be of significant importance for developing new strategies for the prevention and treatment of both UF and AH [29], as well as for understanding the common molecular mechanisms underlying these diseases.

6. Study Limitations

This study has several limitations. First, the number of analyzed SNP markers was restricted, which may have limited the scope of genetic associations identified. Second, the use of TaqMan probe-based genotyping imposed methodological constraints, resulting in the exclusion of certain SNPs due to difficulties in probe design. Third, certain clinical variables were either missing for some participants or characterized by low prevalence, which limited our ability to explore gene–environment interactions and the potential influence of SNPs on specific clinical features of the disease. Finally, the principal limitations of this research involve the modest cohort size and the necessity for validation across different ethnic populations.

Availability of Data and Materials

The original contributions presented in the study are included in the article/**Supplementary Material**, further inquiries can be directed to the corresponding author.

Author Contributions

OB designed the research study. LP, JS and AD performed the experiments. LP, KK, and OB analyzed the data. LP and OB wrote the manuscript. All authors contributed to editorial changes in the manuscript. All authors read and approved the final manuscript. All authors have participated sufficiently in the work and agreed to be accountable for all aspects of the work.

Ethics Approval and Consent to Participate

The research protocol was approved by the Ethics Committee of Kursk State Medical University (protocol number 5, from May 11, 2021). This research complied with all ethical standards outlined in the Declaration of Helsinki and was performed in full adherence to applicable national regulations and institutional policy requirements. All of the participants provided signed informed consent.

Acknowledgment

Not applicable.

Funding

This research received no external funding.

Conflict of Interest

The authors declare no conflict of interest.

Declaration of AI and AI-Assisted Technologies in the Writing Process

In the course of manuscript preparation, the authors employed Microsoft Copilot and DeepL to improve text clarity and check grammar. All outputs generated with these tools were carefully reviewed and revised by the authors, who assume full responsibility for the final content of the publication.

Supplementary Material

Supplementary material associated with this article can be found, in the online version, at https://doi.org/10.31083/FBS42728.

References

[1] Fedotova M, Barysheva E, Bushueva O. Pathways of Hypoxia-Inducible Factor (HIF) in the Orchestration of Uterine Fibroids Development. Life (Basel, Switzerland). 2023; 13: 1740. https://doi.org/10.3390/life13081740.

[2] Pavone D, Clemenza S, Sorbi F, Fambrini M, Petraglia F. Epidemiology and Risk Factors of Uterine Fibroids. Best Practice & Research. Clinical Obstetrics & Gynaecology. 2018; 46: 3–11. https://doi.org/10.1016/j.bpobgyn.2017.09.004.

[3] Giuliani E, As-Sanie S, Marsh EE. Epidemiology and management of uterine fibroids. International Journal of Gynaecology and Obstetrics: the Official Organ of the International Federation of Gynaecology and Obstetrics. 2020; 149: 3–9. https://doi.org/10.1002/ijgo.13102.

[4] Dai Y, Chen H, Yu J, Cai J, Lu B, Dai M, *et al*. Global and regional trends in the incidence and prevalence of uterine fibroids and attributable risk factors at the national level from 2010 to 2019: A worldwide database study. Chinese Medical Journal. 2024; 137: 2583-2589. https://doi.org/10.1097/cm9.0000000000002971.

[5] Lou Z, Huang Y, Li S, Luo Z, Li C, Chu K, *et al*. Global, regional, and national time trends in incidence, prevalence, years lived with disability for uterine fibroids, 1990-2019: an age-period-cohort analysis for the global burden of disease 2019 study. BMC Public Health. 2023; 23: 916. https://doi.org/10.1186/s12889-023-15765-x.

[6] Mills KT, Stefanescu A, He J. The global epidemiology of hypertension. Nature Reviews. Nephrology. 2020; 16: 223–237. https://doi.org/10.1038/s41581-019-0244-2.

[7] Stewart EA, Cookson CL, Gandolfo RA, Schulze-Rath R. Epidemiology of uterine fibroids: a systematic review. BJOG: an International Journal of Obstetrics and Gynaecology. 2017; 124: 1501–1512. https://doi.org/10.1111/1471-0528.14640.

[8] Haan Y, De Lange ME, Suhooli HJM, Ankum WM, Timmermans TA, Limpens J, *et al*. PP.16.16: The association between hypertension and uterine fibroids a systematic review and meta-analysis. Journal of Hypertension. 2015; 33: e274. https://doi.org/10.1097/01.hjh.0000468197.95949.02.

[9] Chen Y, Xiong N, Xiao J, Huang X, Chen R, Ye S, *et al*. Association of uterine fibroids with increased blood pressure: a cross-sectional study and meta-analysis. Hypertension Research: Official Journal of the Japanese Society of Hypertension. 2022; 45: 715–721. https://doi.org/10.1038/s41440-022-00856-w.

[10] Chen Y, Lin M, Guo P, Xiao J, Huang X, Xu L, *et al*. Uterine fibroids increase the risk of hypertensive disorders of pregnancy: a prospective cohort study. Journal of Hypertension. 2021; 39: 1002–1008. https://doi.org/10.1097/HJH.0000000000002729.

[11] Nasab S, Gough EK, Nylander E, Borahay M, Segars J, Baker V, *et al*. Uterine Fibroids and Hypertensive Disorders in Pregnancy: A Systematic Review and Meta-Analysis. medRxiv. 2024; 2024.03.05.24303824. https://doi.org/10.1101/2024.03.05.24303824. (preprint)

[12] Lazarenko V, Churilin M, Azarova I, Klyosova E, Bykanova M, Ob'edkova N, *et al*. Comprehensive Statistical and Bioinformatics Analysis in the Deciphering of Putative Mechanisms by Which Lipid-Associated GWAS Loci Contribute to Coronary Artery Disease. Biomedicines. 2022; 10: 259. https://doi.org/10.3390/biomedicines10020259.

[13] Gallagher CS, Mäkinen N, Harris HR, Rahmioglu N, Uimari O, Cook JP, *et al*. Genome-wide association and epidemiological analyses reveal common genetic origins between uterine leiomyomata and endometriosis. Nature Communications. 2019; 10: 4857. https://doi.org/10.1038/s41467-019-12536-4.

[14] Edwards TL, Giri A, Hellwege JN, Hartmann KE, Stewart EA, Jeff JM, *et al*. A *Trans*-Ethnic Genome-Wide Association Study of Uterine Fibroids. Frontiers in Genetics. 2019; 10: 511. https://doi.org/10.3389/fgene.2019.00511.

[15] Qu Y, Chen L, Guo S, Liu Y, Wu H. Genetic liability to multiple factors and uterine leiomyoma risk: a Mendelian randomization study. Frontiers in Endocrinology. 2023; 14: 1133260. https://doi.org/10.3389/fendo.2023.1133260.

[16] Ponomareva L, Kobzeva K, Bushueva O. GWAS-Significant Loci and Uterine Fibroids Risk: Analysis of Associations, Gene-Gene and Gene-Environmental Interactions. Frontiers in Bioscience (Scholar Edition). 2024; 16: 24. https://doi.org/10.31083/j.fbs1604024.

[17] Levy D, Ehret GB, Rice K, Verwoert GC, Launer LJ, Dehghan A, *et al*. Genome-wide association study of blood pressure and hypertension. Nature Genetics. 2009; 41: 677–687. https://doi.org/10.1038/ng.384.

[18] Padmanabhan S, Dominiczak AF. Genomics of hypertension: the road to precision medicine. Nature Reviews. Cardiology. 2021; 18: 235–250. https://doi.org/10.1038/s41569-020-00466-4.

[19] Bushueva OY. Single nucleotide polymorphisms in genes encoding xenobiotic metabolizing enzymes are associated with predisposition to arterial hypertension. Research Results in Biomedicine 2020; 6: 447–456. https://doi.org/10.18413/2658-6533-2020-6-4-0-1.

[20] Koressaar T, Remm M. Enhancements and modifications of primer design program Primer3. Bioinformatics (Oxford, England). 2007; 23: 1289–1291. https://doi.org/10.1093/bioinformatics/btm091.

[21] Johnson JL, Abecasis GR. GAS Power Calculator: web-based power calculator for genetic association studies. BioRxiv. 2017; 164343. https://doi.org/10.1101/164343. (preprint)

[22] Ponomarenko I, Pasenov K, Churnosova M, Sorokina I, Aristova I, Churnosov V, *et al*. Sex-Hormone-Binding Globulin Gene Polymorphisms and Breast Cancer Risk in Caucasian Women of Russia. International Journal of Molecular Sciences. 2024; 25: 2182. https://doi.org/10.3390/ijms25042182.

[23] Ivanova TA. Sex-specific features of interlocus interactions determining susceptibility to hypertension. Research Results in Biomedicine. 2024; 10: 53–68. https://doi.org/10.18413/2658-6533-2024-10-1-0-3. (In Russian)

[24] Belykh AE, Soldatov VO, Stetskaya TA, Kobzeva KA, Soldatova MO, Polonikov AV, *et al*. Polymorphism of *SERF2*, the gene encoding a heat-resistant obscure (Hero) protein with chaperone activity, is a novel link in ischemic stroke. IBRO Neuroscience Reports. 2023; 14: 453–461. https://doi.org/10.1016/j.ibneur.2023.05.004.

[25] Kobzeva KA, Shilenok IV, Belykh AE, Gurtovoy DE, Bobyleva, Krapiva AB, *et al*. C9orf16 (BBLN) gene, encoding a member of Hero proteins, is a novel marker in ischemic stroke risk. Research Results in Biomedicine. 2022; 8: 278–292. https://doi.org/10.18413/2658-6533-2022-8-3-0-2.

[26] Shilenok I, Kobzeva K, Deykin A, Pokrovsky V, Patrakhanov E, Bushueva O. Obesity and Environmental Risk Factors Significantly Modify the Association between Ischemic Stroke and the Hero Chaperone *C19orf53*. Life (Basel, Switzerland). 2024; 14: 1158. https://doi.org/10.3390/life14091158.

[27] Stetskaya TA, Kobzeva KA, Zaytsev SM, Shilenok IV, Komkova GV, Goryainova NV, *et al*. HSPD1 gene polymorphism is associated with an increased risk of ischemic stroke in smokers. Research Results in Biomedicine. 2024; 10: 175–186. https://doi.org/10.18413/2658-6533-2024-10-2-0-1.

[28] Shilenok I, Kobzeva K, Soldatov V, Deykin A, Bushueva O. *C11orf58* (Hero20) Gene Polymorphism: Contribution to Is-

chemic Stroke Risk and Interactions with Other Heat-Resistant Obscure Chaperones. Biomedicines. 2024; 12: 2603. https://doi.org/10.3390/biomedicines12112603.

[29] Stewart EA, Borah BJ. Uterine Fibroids and Hypertension: Steps Toward Understanding the Link. The Journal of Clinical Endocrinology and Metabolism. 2021; 106: e1039–e1041. https://doi.org/10.1210/clinem/dgaa829.

[30] Brewster LM, Perrotta ID, Jagernath Z, Taherzadeh Z, van Montfrans GA. Ultrastructural changes in resistance arterioles of normotensive and hypertensive premenopausal women with uterine fibroids. Ultrastructural Pathology. 2023; 1–12. https://doi.org/10.1080/01913123.2023.2171168.

[31] Te Riet L, van Esch JHM, Roks AJM, van den Meiracker AH, Danser AHJ. Hypertension: renin-angiotensin-aldosterone system alterations. Circulation Research. 2015; 116: 960–975. https://doi.org/10.1161/CIRCRESAHA.116.303587.

[32] Keshavarzi F, Teimoori B, Farzaneh F, Mokhtari M, Najafi D, Salimi S. Association of ACE I/D and AGTR1 A1166C Gene Polymorphisms and Risk of Uterine Leiomyoma: A Case-Control Study. Asian Pacific Journal of Cancer Prevention: APJCP. 2019; 20: 2595–2599. https://doi.org/10.31557/APJCP.2019.20.9.2595.

[33] Kirschen GW, Yanek L, Borahay M. Relationship Among Surgical Fibroid Removal, Blood Pressure, and Biomarkers of Renin-Angiotensin-Aldosterone System Activation. Reproductive Sciences (Thousand Oaks, Calif.). 2023; 30: 2736–2742. https://doi.org/10.1007/s43032-023-01215-x.

[34] Isobe A, Takeda T, Wakabayashi A, Tsuiji K, Li B, Sakata M, *et al*. Aldosterone stimulates the proliferation of uterine leiomyoma cells. Gynecological Endocrinology: the Official Journal of the International Society of Gynecological Endocrinology. 2010; 26: 372–377. https://doi.org/10.3109/09513590903511521.

[35] Armanini D, Sabbadin C, Donà G, Bordin L, Marin L, Andrisani A, *et al*. Uterine fibroids and risk of hypertension: Implication of inflammation and a possible role of the renin-angiotensin-aldosterone system. Journal of Clinical Hypertension (Greenwich, Conn.). 2018; 20: 727–729. https://doi.org/10.1111/jch.13262.

[36] Kirschen GW, AlAshqar A, Miyashita-Ishiwata M, Reschke L, El Sabeh M, Borahay MA. Vascular biology of uterine fibroids: connecting fibroids and vascular disorders. Reproduction (Cambridge, England). 2021; 162: R1–R18. https://doi.org/10.1530/REP-21-0087.

[37] Wong JYY, Gold EB, Johnson WO, Lee JS. Circulating Sex Hormones and Risk of Uterine Fibroids: Study of Women's Health Across the Nation (SWAN). The Journal of Clinical Endocrinology and Metabolism. 2016; 101: 123–130. https://doi.org/10.1210/jc.2015-2935.

[38] Alsudairi H, Alrasheed A, Dvornyk V. Estrogens and uterine fibroids: an integrated view. Research Results in Biomedicine. 2021; 7: 156–163. https://doi.org/10.18413/2658-6533-2021-7-2-0-6.

[39] Reis FM, Bloise E, Ortiga-Carvalho TM. Hormones and pathogenesis of uterine fibroids. Best Practice & Research. Clinical Obstetrics & Gynaecology. 2016; 34: 13–24. https://doi.org/10.1016/j.bpobgyn.2015.11.015.

[40] Visniauskas B, Kilanowski-Doroh I, Ogola BO, Mcnally AB, Horton AC, Imulinde Sugi A, *et al*. Estrogen-mediated mechanisms in hypertension and other cardiovascular diseases. Journal of Human Hypertension. 2023; 37: 609–618. https://doi.org/10.1038/s41371-022-00771-0.

[41] Lin Y, Chen Z, Kato S. Receptor-selective IL-4 mutein modulates inflammatory vascular cell phenotypes and attenuates atherogenesis in apolipoprotein E-knockout mice. Experimental and Molecular Pathology. 2015; 99: 116–127. https://doi.org/10.1016/j.yexmp.2015.06.007.

[42] Satou R, Gonzalez-Villalobos RA. JAK-STAT and the renin-angiotensin system: The role of the JAK-STAT pathway in blood pressure and intrarenal renin-angiotensin system regulation. JAK-STAT. 2012; 1: 250–256. https://doi.org/10.4161/jkst.22729.

[43] Wagner MA, Siddiqui MAQ. The JAK-STAT pathway in hypertrophic stress signaling and genomic stress response. JAK-STAT. 2012; 1: 131–141. https://doi.org/10.4161/jkst.20702.

[44] Kalinina N, Agrotis A, Antropova Y, Ilyinskaya O, Smirnov V, Tararak E, *et al*. Smad expression in human atherosclerotic lesions: evidence for impaired TGF-beta/Smad signaling in smooth muscle cells of fibrofatty lesions. Arteriosclerosis, Thrombosis, and Vascular Biology. 2004; 24: 1391–1396. https://doi.org/10.1161/01.ATV.0000133605.89421.79.

[45] Beenken A, Mohammadi M. The FGF family: biology, pathophysiology and therapy. Nature Reviews. Drug Discovery. 2009; 8: 235–253. https://doi.org/10.1038/nrd2792.

[46] Zhang P, Zhang H, Wang Y. FGFR4 promotes nuclear localization of GABP to inhibit cell apoptosis in uterine leiomyosarcoma. Cell and Tissue Research. 2021; 383: 865–879. https://doi.org/10.1007/s00441-020-03296-5.

[47] Stolk L, Perry JRB, Chasman DI, He C, Mangino M, Sulem P, *et al*. Meta-analyses identify 13 loci associated with age at menopause and highlight DNA repair and immune pathways. Nature Genetics. 2012; 44: 260–268. https://doi.org/10.1038/ng.1051.

[48] Anagnostis P, Theocharis P, Lallas K, Konstantis G, Mastrogiannis K, Bosdou JK, *et al*. Early menopause is associated with increased risk of arterial hypertension: A systematic review and meta-analysis. Maturitas. 2020; 135: 74–79. https://doi.org/10.1016/j.maturitas.2020.03.006.

[49] Lin YH, Wu Y, Wang Y, Yao ZF, Tang J, Wang R, *et al*. Spatiotemporal expression of Hexokinase-3 in the injured female rat spinal cords. Neurochemistry International. 2018; 113: 23–33. https://doi.org/10.1016/j.neuint.2017.11.015.

[50] Kuwabara M, Chintaluru Y, Kanbay M, Niwa K, Hisatome I, Andres-Hernando A, *et al*. Fasting blood glucose is predictive of hypertension in a general Japanese population. Journal of Hypertension. 2019; 37: 167–174. https://doi.org/10.1097/HJH.0000000000001895.

[51] Guzik TJ, Nosalski R, Maffia P, Drummond GR. Immune and inflammatory mechanisms in hypertension. Nature Reviews. Cardiology. 2024; 21: 396–416. https://doi.org/10.1038/s41569-023-00964-1.

[52] Andrade J, Shi C, Costa ASH, Choi J, Kim J, Doddaballapur A, *et al*. Control of endothelial quiescence by FOXO-regulated metabolites. Nature Cell Biology. 2021; 23: 413–423. https://doi.org/10.1038/s41556-021-00637-6.

[53] Yu W, Chen C, Cheng J. The role and molecular mechanism of FoxO1 in mediating cardiac hypertrophy. ESC Heart Failure. 2020; 7: 3497–3504. https://doi.org/10.1002/ehf2.13065.

[54] Palmieri F, Scarcia P, Monné M. Diseases Caused by Mutations in Mitochondrial Carrier Genes *SLC25*: A Review. Biomolecules. 2020; 10: 655. https://doi.org/10.3390/biom10040655.

[55] Zhang Q, Wei T, Jin W, Yan L, Shi L, Zhu S, *et al*. Deficiency in SLC25A15, a hypoxia-responsive gene, promotes hepatocellular carcinoma by reprogramming glutamine metabolism. Journal of Hepatology. 2024; 80: 293–308. https://doi.org/10.1016/j.jhep.2023.10.024.

[56] Griendling KK, Camargo LL, Rios FJ, Alves-Lopes R, Montezano AC, Touyz RM. Oxidative Stress and Hypertension. Circulation Research. 2021; 128: 993–1020. https://doi.org/10.1161/CIRCRESAHA.121.318063.

[57] Lahera V, de Las Heras N, López-Farré A, Manucha W, Ferder L. Role of Mitochondrial Dysfunction in Hypertension and Obesity. Current Hypertension Reports. 2017; 19: 11. https://doi.org/10.1007/s11906-017-0710-9.

[58] Bushueva O, Barysheva E, Markov A, Belykh A, Koroleva I, Churkin E, *et al*. DNA Hypomethylation of the MPO Gene in Peripheral Blood Leukocytes Is Associated with Cerebral Stroke in the Acute Phase. Journal of Molecular Neuroscience: MN. 2021; 71: 1914–1932. https://doi.org/10.1007/s12031-021-01840-8.

[59] Soldatov V, Venediktov A, Belykh A, Piavchenko G, Naimzada MD, Ogneva N, *et al*. Chaperones vs. oxidative stress in the pathobiology of ischemic stroke. Frontiers in Molecular Neuroscience. 2024; 17: 1513084. https://doi.org/10.3389/fnmol.2024.1513084.

[60] Jozwik KM, Held JP, Hecht CA, Patel MR. A viable hypomorphic mutation in the mitochondrial ribosome subunit, MRPS-31, exhibits mitochondrial dysfunction in *C. elegans*. MicroPublication Biology. 2024; 2024: 10.17912/micropub.biology.001344. https://doi.org/10.17912/micropub.biology.001344.

[61] Engal E, Oja KT, Maroofian R, Geminder O, Le TL, Mor E, *et al*. Biallelic loss of function variants in WBP4, encoding a spliceosome protein, result in a variable neurodevelopmental delay syndrome. The American Journal of Human Genetics. 2023; 110: 2112–2119. https://doi.org/10.1016/j.ajhg.2023.10.013.

[62] Yang L, Wang B, Zhou Q, Wang Y, Liu X, Liu Z, *et al*. MicroRNA-21 prevents excessive inflammation and cardiac dysfunction after myocardial infarction through targeting KBTBD7. Cell Death & Disease. 2018; 9: 769. https://doi.org/10.1038/s41419-018-0805-5.

[63] Fang Y, Xu Y, Wang R, Hu L, Guo D, Xue F, *et al*. Recent advances on the roles of LncRNAs in cardiovascular disease. Journal of Cellular and Molecular Medicine. 2020; 24: 12246–12257. https://doi.org/10.1111/jcmm.15880.

[64] Melton E, Qiu H. Interleukin-1β in Multifactorial Hypertension: Inflammation, Vascular Smooth Muscle Cell and Extracellular Matrix Remodeling, and Non-Coding RNA Regulation. International Journal of Molecular Sciences. 2021; 22: 8639. https://doi.org/10.3390/ijms22168639.

[65] Kamide K, Kokubo Y, Yang J, Tanaka C, Hanada H, Takiuchi S, *et al*. Hypertension susceptibility genes on chromosome 2p24-p25 in a general Japanese population. Journal of Hypertension. 2005; 23: 955–960. https://doi.org/10.1097/01.hjh.0000166835.70935.3c.

[66] Chamarthi B, Williams GH, Ricchiuti V, Srikumar N, Hopkins PN, Luther JM, *et al*. Inflammation and hypertension: the interplay of interleukin-6, dietary sodium, and the renin-angiotensin system in humans. American Journal of Hypertension. 2011; 24: 1143–1148. https://doi.org/10.1038/ajh.2011.113.

[67] Luo R, Zhang W, Zhao C, Zhang Y, Wu H, Jin J, *et al*. Elevated Endothelial Hypoxia-Inducible Factor-1α Contributes to Glomerular Injury and Promotes Hypertensive Chronic Kidney Disease. Hypertension (Dallas, Tex.: 1979). 2015; 66: 75–84. https://doi.org/10.1161/HYPERTENSIONAHA.115.05578.

[68] Isobe S, Kataoka M, Endo J, Moriyama H, Okazaki S, Tsuchihashi K, *et al*. Endothelial-Mesenchymal Transition Drives Expression of CD44 Variant and xCT in Pulmonary Hypertension. American Journal of Respiratory Cell and Molecular Biology. 2019; 61: 367–379. https://doi.org/10.1165/rcmb.2018-0231OC.

[69] Yu WH, Woessner JF, Jr, McNeish JD, Stamenkovic I. CD44 anchors the assembly of matrilysin/MMP-7 with heparin-binding epidermal growth factor precursor and ErbB4 and regulates female reproductive organ remodeling. Genes & Development. 2002; 16: 307–323. https://doi.org/10.1101/gad.925702.

[70] Lim B, Jung K, Gwon Y, Oh JG, Roh JI, Hong SH, *et al*. Cardioprotective role of APIP in myocardial infarction through ADORA2B. Cell Death & Disease. 2019; 10: 511. https://doi.org/10.1038/s41419-019-1746-3.

[71] Zhao X, Feng D, Wang Q, Abdulla A, Xie XJ, Zhou J, *et al*. Regulation of lipogenesis by cyclin-dependent kinase 8-mediated control of SREBP-1. The Journal of Clinical Investigation. 2012; 122: 2417–2427. https://doi.org/10.1172/JCI61462.

[72] Islam MS, Greco S, Janjusevic M, Ciavattini A, Giannubilo SR, D'Adderio A, *et al*. Growth factors and pathogenesis. Best Practice & Research. Clinical Obstetrics & Gynaecology. 2016; 34: 25–36. https://doi.org/10.1016/j.bpobgyn.2015.08.018.